



## Factors Affecting of Porous Properties of Carbon Gel Microsphere

**M. A. Elsayed**

Department of Chemical Engineering, Military Technical College, Cairo, Egypt  
Phone: (+201141750544)

E-mail address: [aboelfotoh@gmail.com](mailto:aboelfotoh@gmail.com)

### ABSTRACT

Carbon microsphere with high porosity and surface area were synthesized via the sol-gel polycondensation of resorcinol with formaldehyde in a slightly basic medium and followed by drying and pyrolysis. The effects of different parameters during synthesis were investigated. The porous properties of carbon microsphere were evaluated by nitrogen adsorption method and scanning electron microscopy (SEM). By changing both the catalyst species and resorcinol to catalyst ratio (R/C), it was possible to prepare ultramicroporous carbon sphere with pore size about 1.8 nm. The samples evolve from micro-mesoporous solid (RF-Na<sub>2</sub>CO<sub>3</sub>: combination of types I and IV isotherms) with 24.2% micropore to an exclusively microporous material (RF-NH<sub>4</sub>HCO<sub>3</sub>: type I isotherm) with 98.7% micropore. The results show that it is possible to tailor the morphology of these materials by varying the initial pH of the precursor's solution in a narrow range and that the micropore surface area and micropore volume are independent from the initial pH, while the BET surface area vary from 582 m<sup>2</sup>/g (pH = 3.2) to 680 m<sup>2</sup>/g (pH = 6). However, as the pH increases over pH = 6 the surface area is decreases. These materials can be used as packing for separation columns or as catalysts supports.

**Keywords:** carbon microsphere, sol-gel polycondensation, base catalysts, nitrogen adsorption

## **1. INTRODUCTION**

Porous, activated carbons have been applied in various areas including gas separation, water purification, catalyst supports and electrodes for batteries and fuel cells. Most commercial grade activated carbons are derived from naturally occurring carbonaceous materials such as cook and coconut shell [1, 2]. Activated carbons are synthesized through physical or chemical activation processes of these precursors [3, 4]. Carbons prepared from polymers have structure similar to those in coals but contain fewer mineral impurities [5].

Sol-gel process is a chemical synthesis method extensively applied to the preparation of numerous materials with different chemical structure and properties, such as glasses, ceramics, adsorbents and catalyst supports. Carbon materials derived from polycondensation of hydroxylated benzene (phenol, catechol, resorcinol, hydroquinone,...) and aldehyde (formaldehyde, furfural,...) in a solvent through a reaction mechanism similar to the sol-gel processing followed by drying and pyrolysis have been extensively studied [5]. Organic aerogels syntheses were first introduced by using supercritical drying conditions [6]. Since then, numerous articles have been published on the properties and potential uses of pyrolyzed organic gels [7-9].

Supercritical drying conditions suppress the liquid-vapor interface, avoiding shrinkage and cracking of the material during solvent removal and preserving the porous nature [4]. Supercritical drying is difficult to apply at an industrial scale because it is expensive and potentially dangerous. Residual surface tension and shrinkage are not avoided when the pore size is small or when the material density is low. Another way to avoid liquid-vapour interfaces is to use freeze-drying. After freezing, the solvent is removed by sublimation under low pressure and a 'cryogel' is obtained. Freeze-drying results in an aerogel with mesoporous texture with good cohesion and can handled without breaking up the pores which extend from the nanometre to micrometer length-scale [10, 11].

Monoliths are very difficult to obtain by freeze-drying and the appearance of huge channels due to ice crystal growth at high dilution ratio hinders the fabrication of low density materials. Evaporative drying is suitable when dense carbons are needed or when the only selection criterion is the micropore size. Indeed, very porous carbon materials can be obtained by direct evaporative drying and pyrolysis of aqueous resorcinol-formaldehyde gels provided that the operating variables are correctly chosen. Surprising, this very simple method is rarely used and more complicated drying techniques are being used [4].

Few works published in literature concern evaporative drying leading to the obtaining of materials called 'microsphere'. In this case, solvent exchange is always used in order to reduce the capillary forces responsible for the pore texture destruction. Many researchers have devoted their efforts to create or tailor the desired pore properties [12]. In previous work, sodium carbonate was used as basification agent. The primary role of the  $\text{Na}_2\text{CO}_3$  is to increase the pH of the resorcinol-formaldehyde aqueous solution. In fact, the true synthesis variable is the pH of the starting solution, and the pH adjustment can be achieved by addition of any base [13].

The objectives of the current work is to further develop and modify resorcinol formaldehyde sol-gel synthesis procedure to make high surface area carbon microsphere with a controlled pore structure. In this paper, we experimentally elucidate the influence of the amount of catalyst, diluents and the initial pH of the PF solution on the surface area, pore

volume, and pore size distribution by Nitrogen adsorption. The results are presented; along with results obtained from SEM, TGA and FTIR.

## **2. EXPERIMENTAL**

### **2. 1. Resin synthesis**

RF hydrogel were synthesized by the polycondensation of resorcinol (P) (1,3 dihydroxybenzene  $C_6H_4(OH)_2$ ) (reagent-grade 98%, Aldrich) and formaldehyde (F) (HCHO) (37% in water, stabilized by 10-15% wt. methanol, Aldrich) using initial R/F molar ratio of 1:2. Deionised water (W) was used as the diluent. Monoethanolamine (MEA), diethanolamine (DEA), methyldiethanoamine (MDEA), ammonium hydrogen carbonate ( $NH_4HCO_3$ ), potassium carbonate ( $K_2CO_3$ ) (research grade, Aldrich), as well as sodium carbonate ( $Na_2CO_3$ ), were also used as catalysts. Each resin has been designated using the nomenclature of its resin type (PF), followed by the catalytic species used. After dissolution of the resorcinol/water mixture, formaldehyde was added and the pH value was then adjusted by addition of diluted solution (2N and 0.5N) of  $HNO_3$ . The use of two different diluted solutions of various concentrations enable to minimize the amount of water added during pH adjustment. The mixture was then stirred for 15 minutes. The vials were sealed and gelation was performed at 85 °C in an oven for three days.

### **2. 2. Preparation of PF microspheres**

In order to increase the crosslinking density by promoting the progress of the condensation reaction of the hydroxymethyl groups, 5% acetic acid was added to the solvent during the initial water to solvent exchange. The excess water was then removed from the gel by acetone for 1 day and by cyclohexane for another day. The solvent was then removed from the pores of the gel slowly, first by evaporating at 60 °C for 2 hours, and then further by exposing it to a vacuum at 120 °C for 12 hours. The functional groups in the resins were qualitatively analyzed with Fourier transform infrared spectrometry (FTIR; Perkin Elmer) using KBr.

### **2. 3. preparation of carbon microspheres**

The RF microsphere was placed in a ceramic boat, pyrolyzed at 850 °C under Argon flow (100 ml/min) in a tubular oven. The pyrolysis conditions were determined by the thermogravimetric analysis. A few milligrams of dried gel placed in a microbalance were pyrolyzed under Argon from ambient temperature to 1000 °C with a constant heating rate 5 °C/min.

### **2. 4. Preparation of active carbon microsphere**

After pyrolysis some samples of the resulting carbonized product were chosen to study the influence of heat treatment in  $CO_2$  atmosphere on the surface area and pore volume. Activation was done at temperature 900 °C with heating rate 30 °C/min.  $N_2$  flow was used during heating and cooling steps. Carbons with different degrees of burn-off were prepared by adjusting the time for gasification.

## 2. 5. Carbon characterization

The porous structures of the carbon microsphere were determined by N<sub>2</sub> adsorption-desorption techniques at 77 K using Micromeritics, ASAP 2000 apparatus. The RF-microsphere were first degassed at 110 °C for 12 hours under vacuum, then the isotherm were measured for relative pressure range  $0.01 \leq P/P_0 \leq 0.99$ . The Brunauer-Emmett-Teller (BET) analysis was performed for relative pressure between  $0.06 \leq P/P_0 \leq 0.2$ . Total pore volume was calculated from the amount of vapor adsorbed at relative pressure of (0.975). Following the IUPAC nomenclature, the pore sizes 2 nm and 50 nm were taken as the limits between micro-and mesopores and meso-and macropores, respectively. Horvath-Kawazoe and BJH model were used to investigate micropore and mesopores size distribution respectively. The micropore volume was calculated from the amount of N<sub>2</sub> adsorbed at relative pressure ( $P_r = P/P_0$ ) of 0.2, and the mesopores volume was calculated by subtractions the amount adsorbed at relative pressure of 0.2 from that adsorbed at relative pressure of 0.99. The average pore diameter was calculated from (4V/A by BET) equation [1,14].

## 3. RESULT AND DISCUSSION

### 3. 1. Resin analysis

#### 3. 1. 1. Ultimate and proximate analysis

After drying, the gels are generally monolithic despite a significant shrinkage. The proximate and ultimate analyses of the cured dried resins were measured using a Thermogravimetric analyzer (TGA; Perkin Elmer TGA 7) and elemental analyzer (Heraeus, CHN-O-RAPID), respectively as shown in Table 1. The proximate analysis was done according to the method described. At ambient temperature in a flow of high purity nitrogen (25 ml min<sup>-1</sup>) approximately 3 mg of the sample is heated to 110 °C at a rate of 150 °C/min and is maintained at this temperature for 1 min. The weight loss is due to water. The sample is further heated to 900 °C at 150 °C/min. and maintained at this temperature for 1 min. This loss is due to volatile matter. Maintaining the temperature at 900 °C the gas is changed to oxygen flowing at 25 ml min<sup>-1</sup>. The weight loss which now occurs is equal to the carbon content, as carbon is burnt off in the oxygen atmosphere. The residual weight corresponds to the ash yield of the sample [15].

**Table 1.** Analysis of resorcinol-formaldehyde resins.

Nomenclature	Ultimate (wt% dry-ash-free basis)				Proximate (wt%)			
	C	H	N	O	Moisture	Volatile	Fixed carbon	Ash
RF-MEA	62.98	5.45	0.42	31.15	4.664	61.796	33.293	0
RF-DEA	64.73	5.24	0.35	29.68	3.397	52.308	43.060	0
RF-MDEA	64.67	5.63	0.31	29.40	2.479	63.733	34.007	0
RF-NH <sub>4</sub> HCO <sub>3</sub>	64.47	4.86	0.32	30.37	2.447	57.133	39.705	0
RF-K <sub>2</sub> CO <sub>3</sub>	63.04	5.12	0.00	31.84	2.292	50.438	45.173	0
RF-Na <sub>2</sub> CO <sub>3</sub>	72.90	6.00	0.00	21.10	3.530	49.675	46.155	0

### 3. 1. 2. Thermo gravimetric analysis

The weight loss versus temperature plot (Fig.1) shows that the sample mass does not change any more above 850 °C, and the derivative plot shows that the quickest mass losses occur at about 110 and 450 °C. All the TG curves indicate a common behaviour; the catalyst species and the catalyst ratios in the synthesis the PF hydrogels do not lead to any great difference in the carbonization process of the PF microsphere. The pyrolysis program was selected so that the heating rate was dwelled after 110, 450 and 650 °C. In addition to, high heating rate could cause a dramatic effect on the pore structure. Thereby, the heating program included the following sequential steps 1) ramp at 0.5 °C/min. to 110 °C and then dwell for 30 min. 2) ramp at 5 °C/min to 450 °C and dwell for 30 min. 3) ramp at 10 °C/min to 850 and dwell for 180 min. 4) cool slowly to room temperature. All the steps were performed under flowing of Ar 100 ml/min.

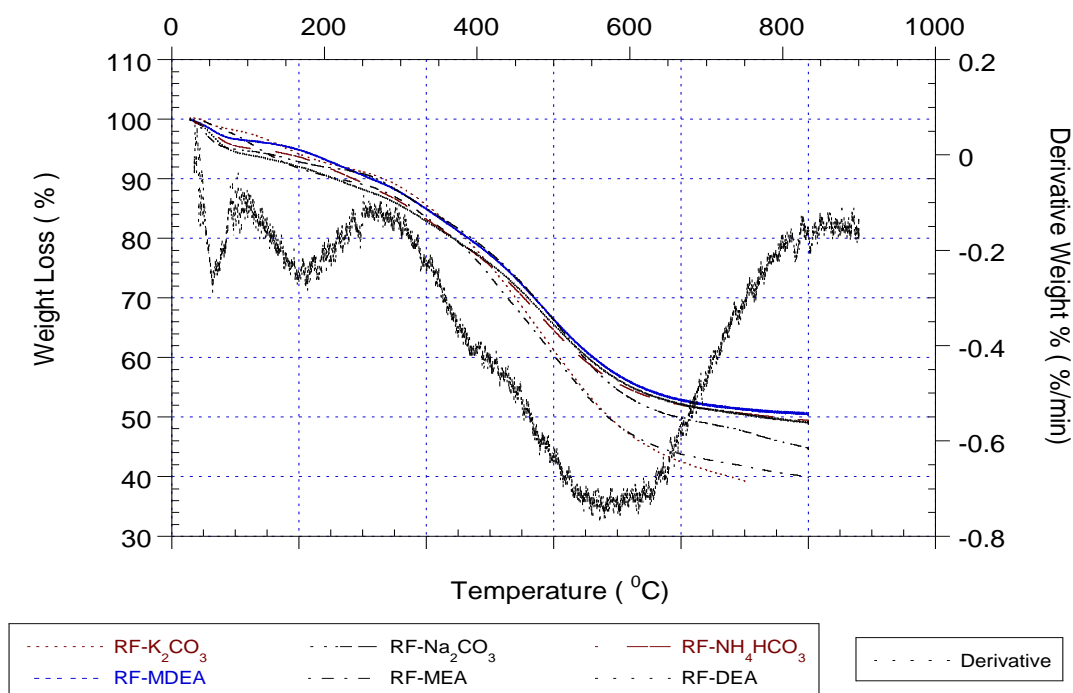


**Figure 1.** Thermogravimetric analysis of a dried resorcinol-formaldehyde gel, % mass losses vs. pyrolysis temperature and derivative plot, heating rate: 5 °C/min.

### 3. 1. 3. FTIR analysis

Fig. 2 Shows the IR spectra for the synthesis resins with different type of catalytic species. The peak at (3570-3200  $\text{cm}^{-1}$ ) is characteristic of -OH groups. The others can not easily be assigned to specific groups. One can assume that the 1460-1480  $\text{cm}^{-1}$  peak corresponds to -CH<sub>2</sub>- group, and that the 1600  $\text{cm}^{-1}$  peak represents aromatic group, C-O-C group should be found between 1000 and 1300  $\text{cm}^{-1}$ , and several peaks appear in this interval.

The main nitrogenated functional groups introduced by the usage of amine and NH<sub>4</sub>HCO<sub>3</sub> as a catalyst in the polycondensation reaction of resorcinol with formaldehyde are

as follows, amides and amines mixed in the very large band around  $3430\text{ cm}^{-1}$ . Nitrile, lactame groups should be found at  $2247\text{ cm}^{-1}$  and  $1730\text{ cm}^{-1}$ , respectively and finally amide group at  $1625\text{ cm}^{-1}$  [7].

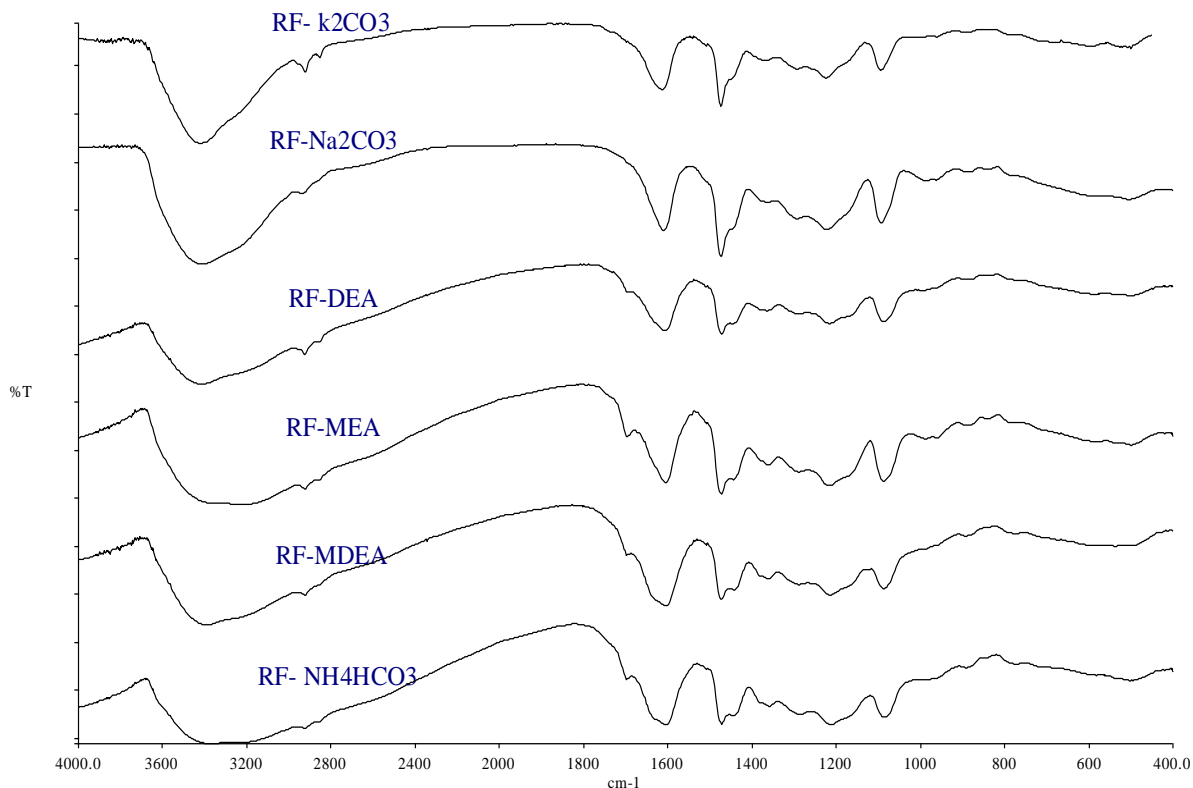


**Figure 2.** FTIR spectra for the synthesis resins with different type of catalytic species and under condition of R/C = 300 by mole, R/W =  $0.25\text{ g/cm}^3$  and pH = 6.

### 3. 2. Pore structure of RF carbon microsphere

#### 3. 2. 1. Effect of changing catalyst species and the catalyst ratios

The influence of the type of basic catalyst and the resorcinol to catalyst ratio on the texture properties of the produced carbon microsphere was investigated. All samples were prepared under the condition of R/W =  $0.25\text{ g/cm}^3$  and pH = 6 with subcritical drying conditions, followed by carbonization at 1123 K for 180 min. The amount of  $\text{N}_2$  adsorbed is plotted against the relative pressure of  $\text{N}_2$  as shown in Fig. 3a. The samples vary from a micro-macroporous solid (RF- $\text{K}_2\text{CO}_3$ : combination of type I and II isotherms) to micro-mesoporous solid (RF- $\text{Na}_2\text{CO}_3$ : combination of types I and IV isotherms), and then to an exclusively microporous material (RF-MEA, DEA, MDEA,  $\text{NH}_4\text{HCO}_3$ : type I isotherm) [16].

The isotherm for the sample prepared by MEA, DEA, MDEA, and  $\text{NH}_4\text{HCO}_3$  exhibits low-pressure hysteresis, which could be attributed to irreversible up-take of adsorptive molecules in pores of about the same width as that of adsorbate molecules, and/or swelling of non-rigid pore walls [17].



The main feature of such isotherm is the long plateau which is indicative of a relatively small amount of multilayer adsorption on the open surface. Micropore filling may take place either in pores of molecular dimensions (i.e. primary micropore filling) at very low  $P/P_0$  or in wider micropores (co-operative filling) over a range of higher  $P/P_0$  [8]. When  $K_2CO_3$  and  $Na_2CO_3$  were used as a catalyst, the  $N_2$  adsorption isotherms are different; they exhibit a significant increase in adsorption at higher relative pressure.

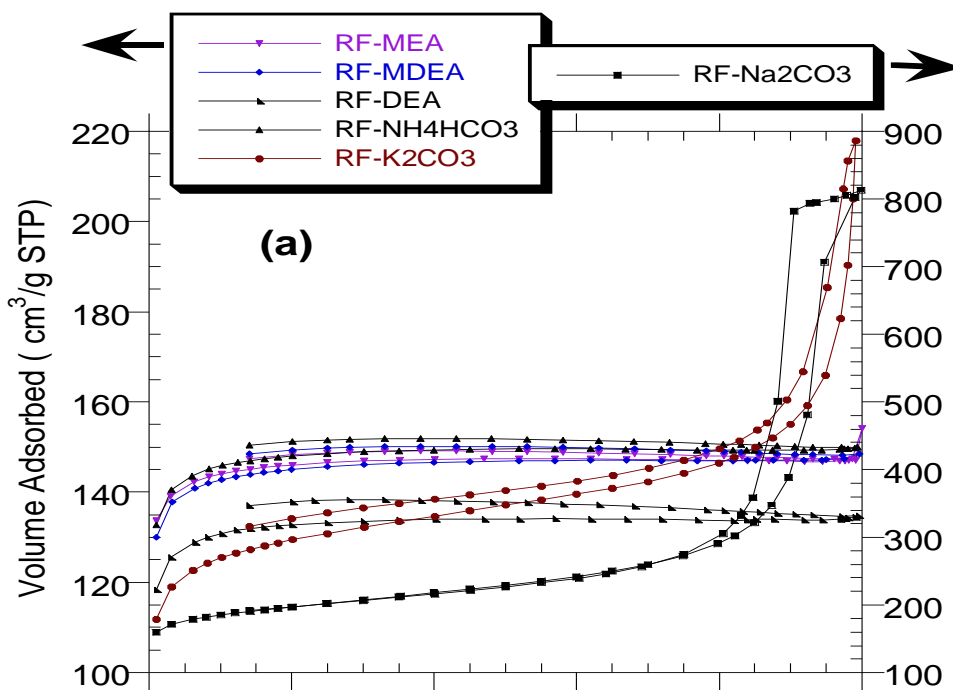
The knee comes to be more open and rounder and the slope of the plateau increases. Also, the nitrogen uptake occurs mostly at ( $P/P_0 > 0.9$ ). This indicates that the meso- or macropore structure in the sample significantly developed.

Fig. 3b shows that as the R/C increases from 50 to 300 the isotherms are shifted from combination of type I and IV isotherms, to type I isotherm with almost horizontal plateau, which extends up to  $P/P_0 > 0.9$ , indicating that the carbon microspheres prepared with ratio  $R/C \geq 300$  are mainly ultramicroporous [12].

The characteristic pore properties of the RF carbon microspheres are listed in Table 2. The specific surface area values vary from  $436 \text{ m}^2/\text{g}$ , (RF- $K_2CO_3$ ), to  $672 \text{ m}^2/\text{g}$ , (RF- $Na_2CO_3$ ). The RF carbon microspheres prepared by  $K_2CO_3$  and  $Na_2CO_3$  as a catalyst are mainly mesoporous, while those prepared by amine and  $NH_4HCO_3$  are mainly microporous.

The mesopores volumes vary from  $0.137$  and  $0.954 \text{ cm}^3/\text{g}$  for  $K_2CO_3$  and  $Na_2CO_3$ , respectively to  $0.003$  and  $0.005 \text{ cm}^3/\text{g}$  for DEA and MDEA. The volume fractions of micropores vary from 24%, (RF-  $Na_2CO_3$ ), to 99%, (RF-  $NH_4HCO_3$ ).

The influence of the catalytic ratio is obviously marked. As R/C decreased from 300 to 50 the total pore volume decreases from  $1.127 \text{ cm}^3/\text{g}$ , (RF-MEA50), to  $0.229 \text{ cm}^3/\text{g}$ , (RF-MEA300). The same trend could be observed for the surface area and the mean pore diameter. On the other hand, the micropore volume fraction increases from 26.2%, (RF-MEA50), to 97.8 %, (RF-MEA300), as R/C decreases from 300 to 50.



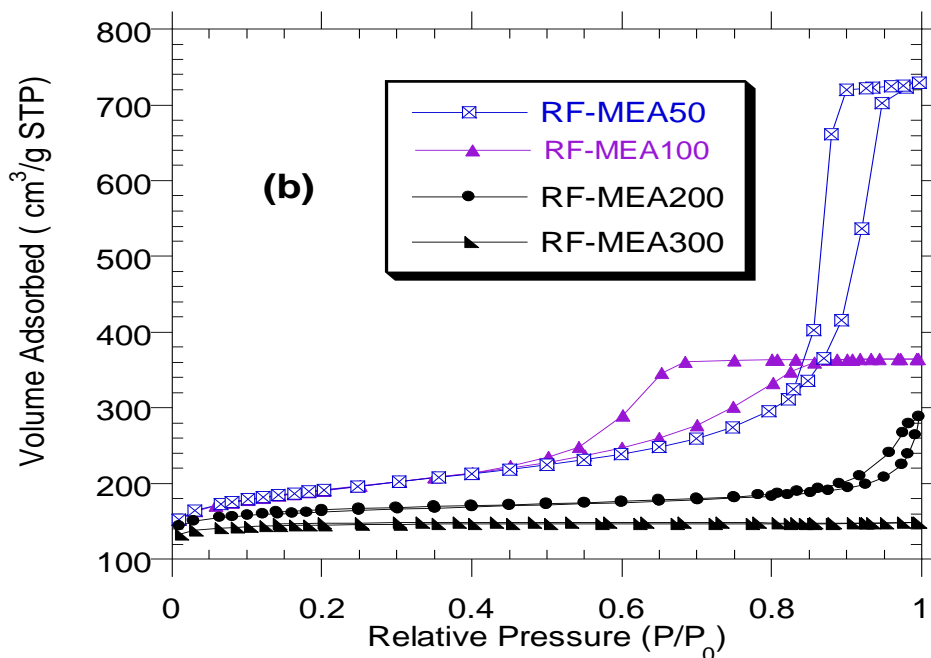


**Figure 3.** Adsorption profiles of  $N_2$  on the RF carbon microsphere generated at a carbonization temperature of 1123 K for 180 min. (a) R/C = 300 with different type of catalytic species (b) MEA was used as a catalyst with different R/C.

Figure 4a and b, illustrate the mesopores size distributions of the RF carbon microsphere synthesized with different catalytic species and those synthesized with different resorcinol to catalyst ratio. The development of the mesoporosity is strongly dependent on the change of the catalyst applied. Fig. 4 a shows that all the samples mainly consist of mesopores less than 5 nm in diameter. An increase in mesopores is observed for the sample prepared by  $K_2CO_3$  and  $Na_2CO_3$ . On the other hand, the sample prepared by amines and  $NH_4HCO_3$  have a peak with maximum intensity at  $\approx 1$  nm. The incremental pore volume increased as the R/C decreased as shown in Fig. 4b. However, the distribution has a single peak for R/C = 50 and 100, while it has some peaks for R/C = 200.

**Table 2.** Characteristic pore properties of RF carbon microsphere.

Nomenclature	R/C	$S_{BET}^a$ ( $m^2/g$ )	$V_t^b$ ( $cm^3/g$ )	$V_{mic}^c$ ( $cm^3/g$ )	$V_{mes}^d$ ( $cm^3/g$ )	$D_p^e$ (nm)	Volume fraction %	
							% micro	% meso
RF- $Na_2CO_3$	300	672	1.258	0.304	0.954	7.476	24.2	75.8
RF- $K_2CO_3$	300	436	0.337	0.200	0.137	3.089	59.3	40.7
RF- $NH_4HCO_3$	300	496	0.232	0.229	0.003	1.870	98.7	1.30
RF-MEA	300	488	0.238	0.226	0.012	1.952	94.9	5.10
RF-DEA	300	444	0.208	0.205	0.003	1.876	98.5	1.50
RF-MDEA	300	485	0.229	0.224	0.005	1.893	97.8	2.20



RF-MEA	50	652	1.127	0.295	0.832	6.914	26.2	73.8
RF-MEA	100	600	0.563	0.295	0.268	3.452	52.4	47.6
RF-MEA	200	546	0.446	0.251	0.195	3.265	56.3	43.7
RF-MEA	300	484	0.229	0.224	0.005	1.899	97.8	2.20

<sup>a</sup> Specific surface area determined from the BET equation, <sup>b</sup>Total pore volume, <sup>c</sup>Micropore volume determine by Horvath-Kawazoe equation, <sup>d</sup>Mesopore volume, <sup>e</sup>Mean pore diameter.

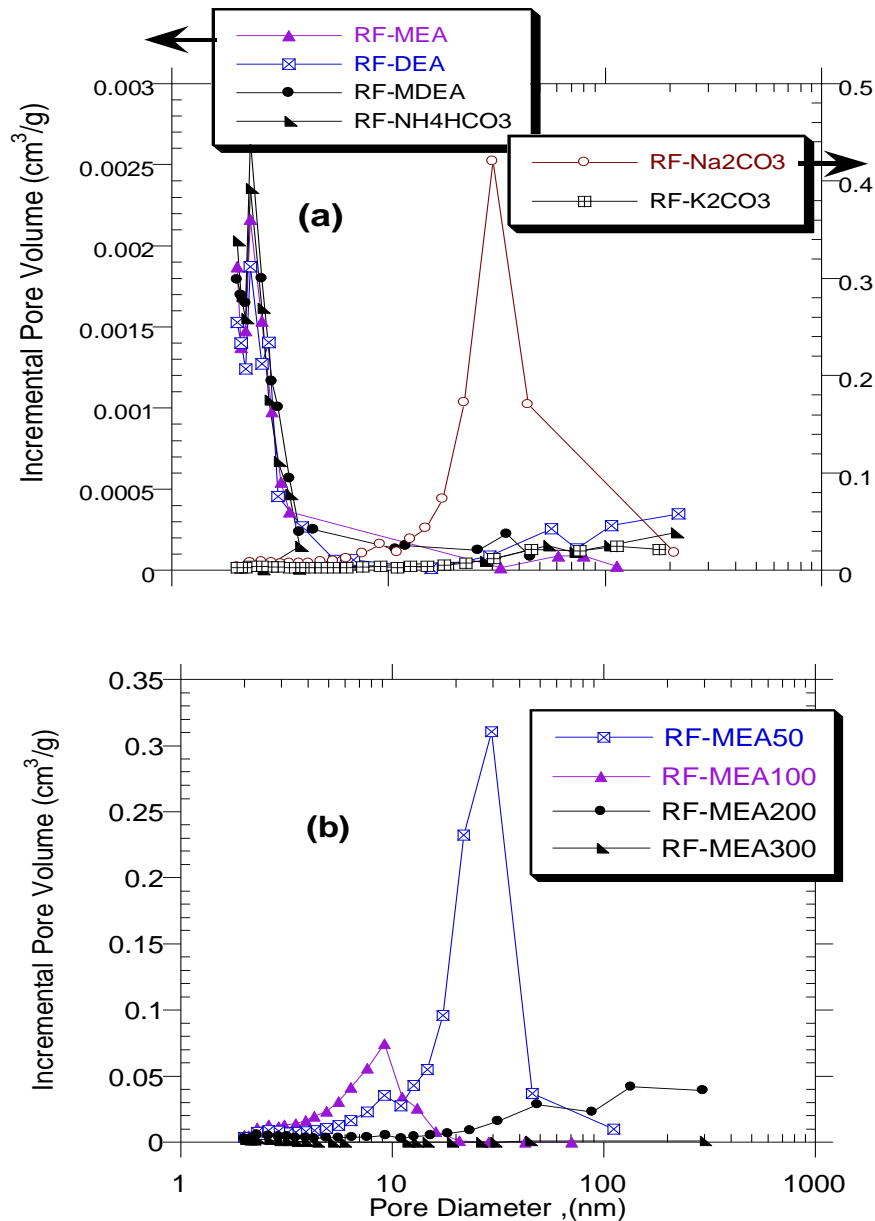


**Figure 4.** Pore size distribution of the RF carbon microspheres generated at a carbonization temperature 1123 K for 180 min. (a) different catalyst species at R/C = 300; (b) different catalyst ratios for the MEA catalyst

### 3. 2. 2. Effect of R/W on porous structure of carbon microsphere

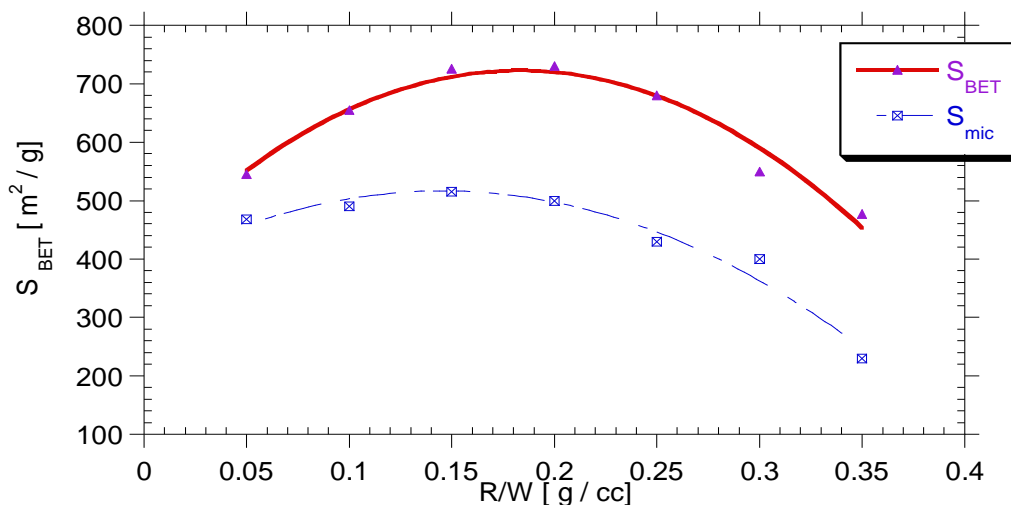


**Figure 5.** Influence of R/W on the BET surface area and micropore surface area of carbon microsphere.

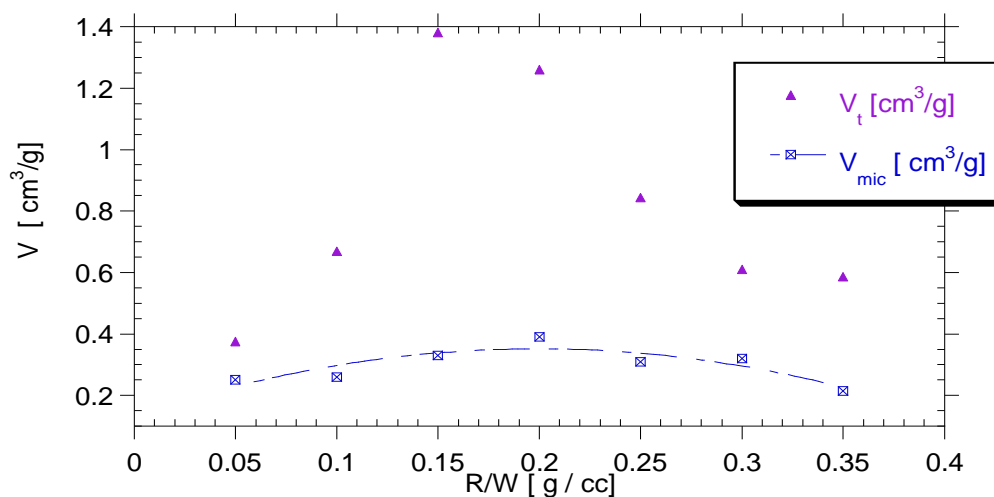


**Figure 6.** Influence of R/W on the total and micro-pore volume of carbon microsphere.

To elucidate the influence of R/W on the porous structure of RF microsphere, the microspheres were prepared using R/C= 100, pH = 6 and MEA as a catalyst. The variations of pore characteristics with R/W of the microspheres prepared are shown in Figures 5-6.  $S_{BET}$  varies from  $545 m^2/g$ , ( $R/W = 0.05 g/cm^3$ ), to  $477 m^2/g$ , ( $R/W = 0.35 g/cm^3$ ), reaching its maximum value  $730 m^2/g$  at ( $R/W = 0.2 g/cm^3$ ). Choosing R/W values lower than 0.05 did not allow the gel to dry. Micropore surface area seems to be independent of R/W in the range of 0.05 to  $0.2 g/cm^3$  and then gradually decreased with increase of R/W, this indicates that at higher R/W values more larger pores are formed which do not contribute too much to the surface area.

The results show that total pore volume  $V_t$  and the micropore volume  $V_{mic}$  have similar R/W dependence as  $S_{BET}$ .

### 3. 2. 3. Effect of pH on the on porous structure of carbon microsphere

Carbon Microsphere were prepared with R/C = 100 by mole, R/W = 0.25 g/cm<sup>3</sup> and MEA as a catalyst. After gelation the gel appearance varied from orange to red brown according to initial pH and catalytic species. Figure 7 shows that  $S_{BET}$  varies from 582 m<sup>2</sup>/g (pH = 3.2) to 680 m<sup>2</sup>/g (pH = 6) indicating that more pores and surface area were created in the RF polymer that remained intact in the carbon microsphere. However, as the pH increases > pH = 6 the surface area is decreased. Furthermore, it was observed that during synthesis, RF gels prepared using an initial pH value higher than 7.3 the gelation was too fast and the gels were sticky and very difficult to filter, while the gels prepared using an initial pH lower than 6.8 were slippery and very easy to filter. It appears that the higher pH yielded gels with a weak chemical structure because fewer, structure-forming condensation reaction occurred. These gels could not withstand the hard drying and pyrolysis conditions which lead to the nanostructure to collapse, leading to carbon microsphere with no or very little surface area. On the other hand, the lower pH promoted the condensation reaction, thereby forming a highly cross-linked and thus very strong structure, where the majority of the pores remained intact even after the high temperature treatment.

Figure 8 shows that the total pore volume increased almost linearly as the pH decreases from 7.3 to 5.2 and then as the pH decreases from 5.2 to 3.2 it remained constant around 1.1 cm<sup>3</sup>/g. Therefore, we could conclude that carbon microsphere evolve from macro-mesoporous solid at lower pH to micro-mesoporous solid at higher pH to completely non-porous material at pH over 7.5 at the specified condition of the preparation.

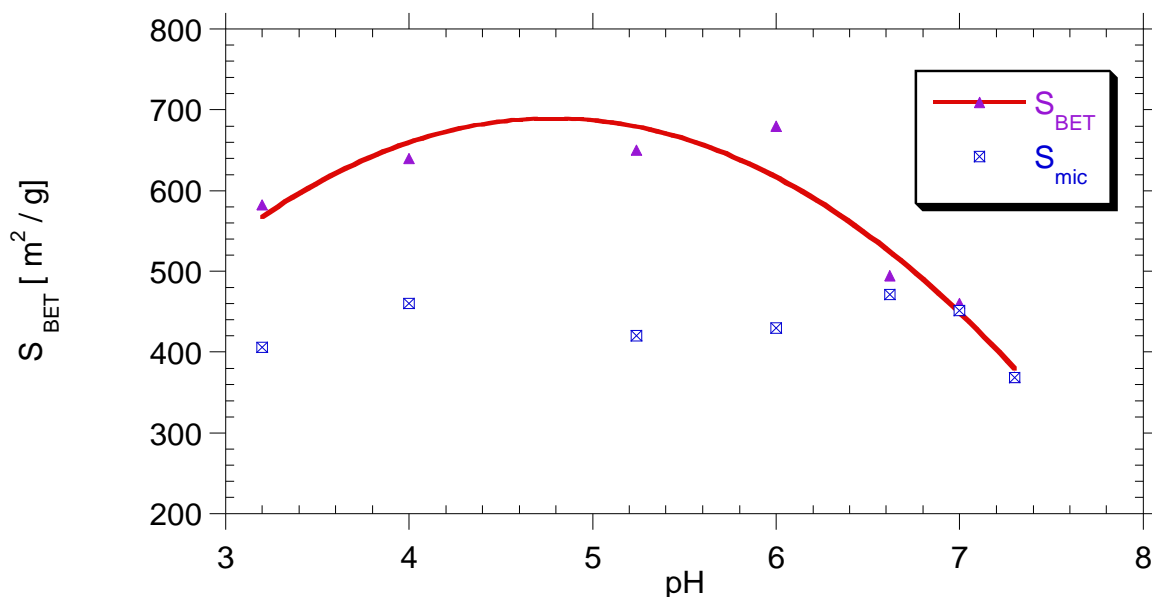


**Figure 7.** Effect of the initial pH of the RF solution on the BET surface area and surface area of micropores.

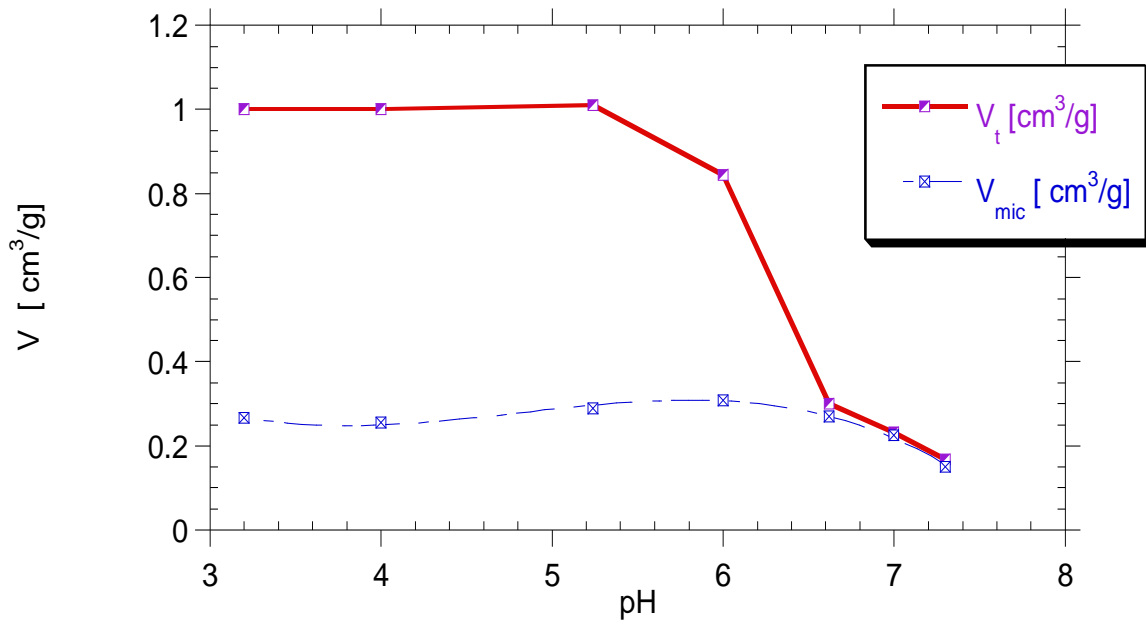


Figure 8. Influence of pH on the total and micro-pores of RF microsphere.

### 3. 2. 4. Effect of Burn-off

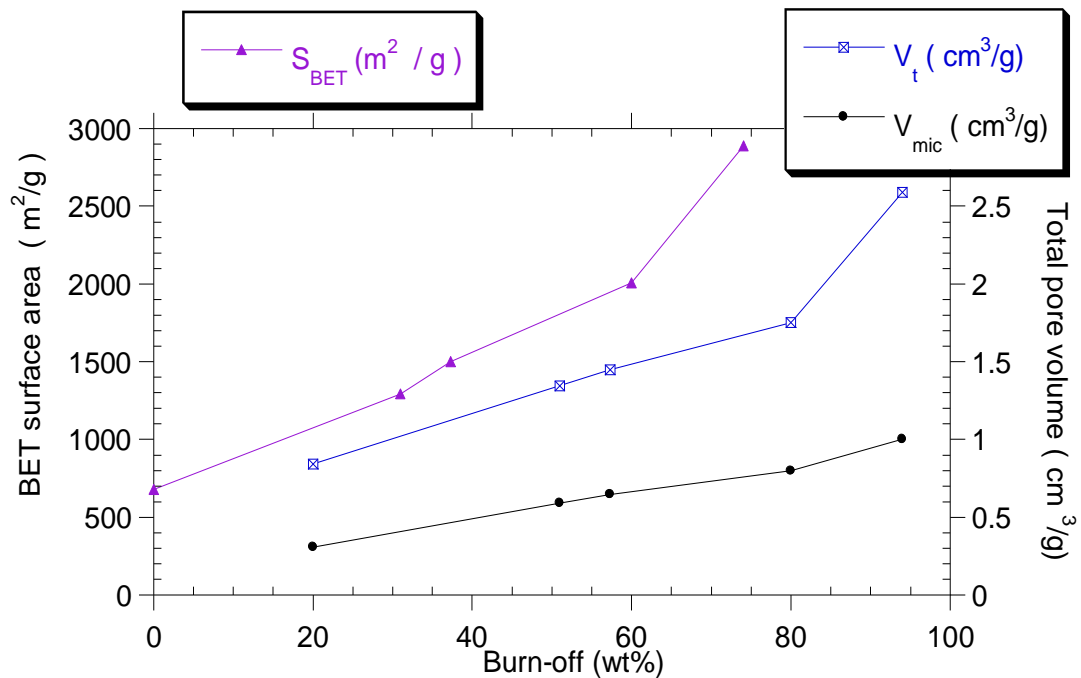
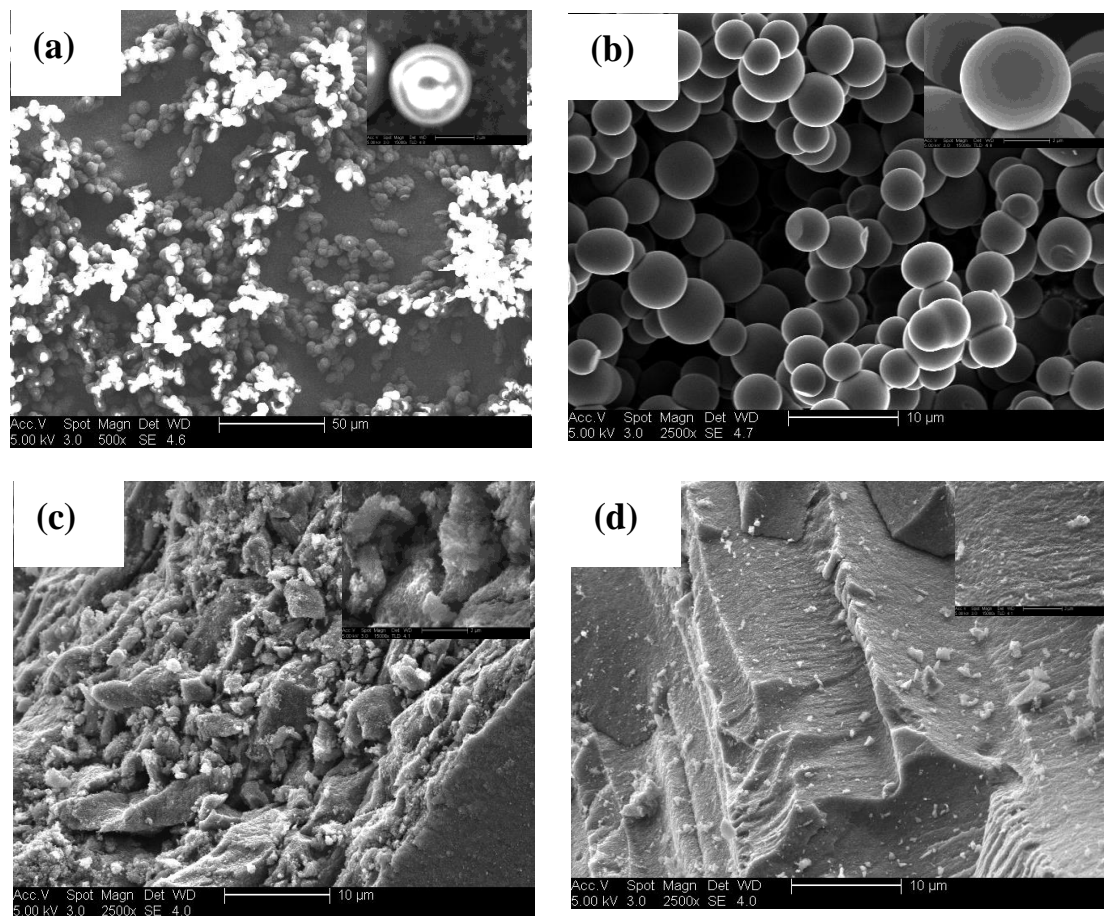


Figure 9. Variation of the BET surface area, pore volume and micropore volume with the burn off level of carbon microsphere gasified in CO<sub>2</sub> at 900 °C.

Pyrolyzed resin prepared with  $R/C = 100$ , MEA as a catalyst,  $pH = 6$  and  $R/W = 0.25$   $g/cm^3$  was subjected to gasification in  $CO_2$ , at  $900\text{ }^\circ C$  for a different period of time to give different burn-off. Figure 9 shows the variation of the surface area and pore volumes with the burn-off level. The porosity increases with the extent of gasification, and high surface area, ( $> 2890\text{ }m^2/g$ ), can be obtained at high burn off levels ( $> 75\%$ ). However, as the degree of burn-off increased the percent of micropore decreased. This can be explained by the fact that removal of carbon atoms from microporous carbons results first in the opening of closed pores, followed by the deepening and enlarging of the micropores, and finally the breaking through of pore walls, resulting in an increase in the number of mesopores. The increase of the surface area with burnoff even at high burnoff levels can be attributed to the endothermic nature of carbon gasification, which could avoid excessive external burning and thus destruction of the microporous structure. However, because of the effect of pore widening, the samples evolve from a micro-mesoporous solid, to a meso-macroporous material.

### 3. 3. Structural characterization with scanning electron microscopy analysis



**Figure 10.** SEM images of cross-section of (a) and (b) samples synthesized under condition  $pH = 6$ ,  $R/C = 30$  and  $R/W = 0.25$  before and after pyrolysis respectively (c) and (d) carbon microsphere synthesized under condition  $pH = 6$ ,  $R/C = 100$  and  $R/W = 0.25$  with 0 % and 37% burn-off respectively. (All the samples were prepared using MEA as catalysis).

Figure 10 a-d show SEM images, each figure contains two different scales images. The SEM images in Figures 10 a and b shows the samples synthesized at pH = 6, R/C = 300 and R/W = 0.25 before and after pyrolysis. There are few differences between the textures obtained before and after pyrolysis despite a mass losses 35-50%.

The SEM suggests that both dried and pyrolyzed materials are made of interconnected spherical particles. Moreover, the particles seem to be more interconnected after pyrolysis and the size of the mesovoids formed between these particles has also decreased. Pictures taken with a higher magnification enabled measurement of an approximate particle diameter. In case of sample after pyrolysis, this diameter increase during pyrolysis from 3.5  $\mu\text{m}$  (polymer before pyrolysis) to 6  $\mu\text{m}$  (carbon particles). Figure 10 c shows the SEM image for the pyrolyzed sample prepared at R/C= 100. The sample reveals interconnected particles with irregular shapes (aggregated particles without a clear boundary). The aggregated particles interlinked together to form three-dimensional network in a particle with a number of mesopores between them. Figure 10 d shows the SEM image for the sample prepared at pH = 6, R/C = 100 and R/W=0.25 and gasified with CO<sub>2</sub> to 37% burn-off value. The sample has a compact structure, enlarging of the micropores and breaking of pore walls were observed, resulting in an increase in the number of mesopores and macropores. The high magnification image shows a surface with a large numbers of small particles distributed over the surface, indicating that most pore development occurs inside the particles.

#### **4. CONCLUSIONS**

This study has demonstrated that microporous carbons with high porosity can be prepared from Resorcinol-Formaldehyde resins. The effects of different parameters during synthesis were investigated. The surface area of carbon microsphere can be controlled by R/C, while the micropore fraction depends on the catalyst used. Na<sub>2</sub>CO<sub>3</sub> produced porous carbons having surface area and pore volumes as high as 672 m<sup>2</sup>/g and 1.26 cm<sup>3</sup>/g, respectively, with micropore fraction 24.2%. A surface area of 488 m<sup>2</sup>/g, pore volume of 0.24 cm<sup>3</sup>/g and micropore fraction 95% can be achieved by using MEA as a catalyst. The mean pore size varied from 1.87 nm (RF-NH<sub>4</sub>HCO<sub>3</sub>) to 7.48 nm (RF-Na<sub>2</sub>CO<sub>3</sub>). Using a pH = 7.1 yielded gels with a weak structure while lower pH = 5 promoted the condensation reaction, thereby forming a highly cross-linked and thus very strong structure. Between an initial pH of 4.8 and 6, the carbon microsphere exhibited the highest surface area of about 680 m<sup>2</sup>/g, with a corresponding pore volume of 0.856 cm<sup>3</sup>/g. The surface area and pore volume are increased with the extent of carbon burn-off FTIR study shows that, samples prepared by MEA, DEA, MDEA and NH<sub>4</sub>HCO<sub>3</sub> contain nitrogenated functional groups. Amides and amines groups are mixed in the very large band around 3430 cm<sup>-1</sup>, nitrile and lactame groups at 2247 cm<sup>-1</sup> and 1730 cm<sup>-1</sup>, respectively. Porous carbon with these functional groups may be suitable candidates for acidic gas capture such as CO<sub>2</sub> and SO<sub>2</sub>.

#### **References**

- [1] H. Jankowska, A. Swiatkowski, J. Choma, T. J. Kemp, Active carbon, Ellis Horwood New York, 1991.

- [2] S. R. Tennison, O. P. Kozynchenko, V. V. Strelko, A. J. Blackburn, US Patent 20,040,024,074, 2004.
- [3] T. Wigmans, *Carbon* 27 (1989) 13-22.
- [4] K. Nakagawa, S. Mukai, K. Tamura, H. Tamon, *Chemical Engineering Research and Design*, 85 (2007) 1331-1337.
- [5] S. Tennison, *Applied Catalysis A: General*, 173 (1998) 289-311.
- [6] R. Pekala, D. Schaefer, *Macromolecules*, 26 (1993) 5487-5493.
- [7] H. Teng, S.-C. Wang, *Carbon*, 38 (2000) 817-824.
- [8] S. Yenisoý-Karakaş, A. Aygün, M. Güneş, E. Tahtasakal, *Carbon*, 42 (2004) 477-484.
- [9] C. Ye, Q.-M. Gong, F.-P. Lu, J. Liang, *Separation and Purification Technology*, 61 (2008) 9-14.
- [10] J.-B. Yang, L.-C. Ling, L. Liu, F.-Y. Kang, Z.-H. Huang, H. Wu, *Carbon*, 40 (2002) 911-916.
- [11] A. Singh, D. Lal, *Journal of Applied Polymer Science*, 100 (2006) 2323-2330.
- [12] K. Lenghaus, G. GuangHua Qiao, D.H. Solomon, C. Gomez, F. Rodriguez-Reinoso, A. Sepulveda-Escribano, *Carbon*, 40 (2002) 743-749.
- [13] M.I. Kim, C.H. Yun, Y.J. Kim, C.R. Park, M. Inagaki, *Carbon*, 40 (2002) 2003-2012.
- [14] P.K. Malik, *Dyes and pigments*, 56 (2003) 239-249.
- [15] M. Smâiések, S. éCernây, *Active carbon: manufacture, properties and applications*, Amsterdam and New York, Elsevier Pub. Co, 1970.
- [16] J. Qiu, Y. Li, Y. Wang, C. Liang, T. Wang, D. Wang, *Carbon*, 41 (2003) 767-772.
- [17] A. Singh, D. Lal, *Journal of Applied Polymer Science*, 110 (2008) 3283-3291.

( Received 10 June 2015; accepted 23 June 2015 )